

REVIEW

Computed tomography-based rigidity analysis: a review of the approach in preclinical and clinical studies

Juan C Villa-Camacho^{1,4}, Otatade Iyoha-Bello^{2,4}, Shohreh Behrouzi^{1,4}, Brian D Snyder^{1,3} and Ara Nazarian¹

¹Center for Advanced Orthopaedic Studies, Beth Israel Deaconess Medical Center, Harvard Medical School, Boston, MA, USA. ²Department of Orthopaedic Surgery, Beth Israel Deaconess Medical Center, Harvard Medical School, Boston, MA, USA. ³Department of Orthopaedic Surgery, Boston Children's Hospital, Harvard Medical School, Boston, MA, USA.

The assessment of fracture risk in patients afflicted with osseous neoplasms has long presented a problem for orthopedic oncologists. These patients are at risk for developing pathologic fractures through lytic defects in the appendicular and axial skeleton with devastating consequences on their quality of life. Lesions with a high risk of fracture may require prophylactic surgical stabilization, whereas low-risk lesions can be treated conservatively. Therefore, effective prevention of pathologic fractures depends on accurate assessment of fracture risk and is a critical step to avoid debilitating complications. Given the complex nature of osseous neoplasms, treatment requires a multidisciplinary approach; yet, little consensus regarding fracture risk assessment exists among physicians involved in the care of these patients. In order to improve the overall standard of care, specific criteria must be adopted to formulate consistent and accurate fracture risk predictions. However, clinicians make subjective assessments about fracture risk on plain radiographs using guidelines now recognized to be inaccurate. Osseous neoplasms alter both the material and geometric properties of bone; failure to account for changes in both of these parameters limits the accuracy of current fracture risk assessments. Rigidity, the capacity to resist deformation upon loading, is a structural property that integrates both the material and geometric properties of bone. Therefore, rigidity can be used as a mechanical assay of the changes induced by lytic lesions to the structural competency of bone. Using this principle, computed tomography (CT)-based structural rigidity analysis (CTRA) was developed and validated in a series of preclinical and clinical studies.

BoneKEy Reports 3, Article number: 587 (2014) | doi:10.1038/bonekey.2014.82

Introduction

The skeleton is the third most common site of metastatic cancer, and nearly half of all cancers metastasize to bone.¹ As a result of new and aggressive treatments, cancer patients are living longer, but at sites of osseous neoplasm fractures occur in up to 35% of affected bones after minimal trauma.² Prevention of pathologic fractures depends on objective criteria that reflect the interaction of the tumor with the host bone. However, clinicians continue to make subjective assessments regarding a patient's fracture risk and response to treatment based on plain radiographs and clinical symptoms now recognized to be inaccurate.³ Osseous neoplasms alter the material and geometric properties of the bone; failure to account for changes in

both of these parameters limits the accuracy of these fracture risk assessments.

Rigidity is a structural property that integrates both the material and geometric properties of bone; the axial (EA), bending (EI) and torsional (GJ) rigidities determine the capacity of the bone to resist axial, bending and twisting loads, respectively. We submit that the structural rigidity of a bone afflicted with cancer provides a mechanical assay that represents the changes in tissue material and geometric properties induced by the disease. On the basis of the principle that it is the *weakest* section that dictates the load capacity for the entire bone, we have developed algorithms to calculate the minimal rigidity of a bone with a neoplastic lesion from serial,

Correspondence: Dr A Nazarian, Center for Advanced Orthopaedic Studies, Beth Israel Deaconess Medical Center, Harvard Medical School, 330 Brookline Avenue, RN115, Boston, MA 2215, USA.

E-mail: anazaria@bidmc.harvard.edu

⁴These authors contributed equally to this work.

Received 4 June 2014; accepted 5 September 2014; published online 5 November 2014

transaxial, computed tomography (CT) images to measure both tissue mineral density and cross-sectional geometry, referred to as CT-based structural rigidity Analysis (CTRA).

Towards a Structural Engineering Approach for Fracture Risk Prediction

As plain radiographs are routinely obtained when treating patients with osseous neoplasms, investigators have tried to estimate the load-bearing capacity (LBC) of a bone from simple radiographic measurements.⁴ Radiographic criteria that rely on measuring defect size only account for the geometry of the defect. However, geometric characterizations of lytic lesions alone do not accurately predict the risk of fracture.⁵ Furthermore, these criteria do not take into consideration the loading mode or the relative location of the defect.

The mechanical behavior of a structure is a function of its material and geometric properties; any method of fracture risk prediction must be able to measure changes in both bone material behavior and bone structural geometry. Current imaging techniques are capable of noninvasive measurements of bone density and cross-sectional geometry. These data, in conjunction with composite beam theory, can be used to predict the LBC of bones with lytic defects. Composite beam theory is an analytical theory that accounts for both the material properties of the individual elements that make up a structure and the overall geometry of the structure itself. Such an approach allows for the estimation of bone structural rigidity, a property defined by the product of the material modulus (which is treated as a function of bone density) and cross-sectional geometry of the structure (**Figure 1**), and it is equivalent to the slope of the linear portion of the load-deformation curve.

In practice, transaxial CT scans of the involved bones (including the lesion and adjacent intact bone) are obtained with a hydroxyapatite (HA) phantom (with three chambers of 0, 500 and 1000 g cm⁻³ HA density) to convert the X-ray attenuation for each pixel to bone mineral density (BMD) and to enable comparison of cases from different imaging sites. Furthermore, the CT images are transformed to be perpendicularly aligned to the neutral axis of the bone of interest in order to obtain true transaxial images. For each transaxial image, EA, EI and GJ are calculated by summing up the modulus-weighted area of each pixel within the bone contour by the position of the pixel relative to the centroid of the bone cross-section. Subsequently, EA, EI and GJ are calculated on each transaxial CT image. In these three rigidities, E is the modulus of elasticity (Young's modulus) of the trabecular or cortical bone, A is the cross-sectional area of the transaxial bone section under consideration, I is the second moment of inertia, G is the torsional modulus of the trabecular or cortical bone and J is the polar moment of inertia. EA provides a measure of the bone's resistance to uniaxial loads; EI provides a measure of the bone's resistance to bending moments; and GJ provides a measure of the bone's resistance to torsional loads.

The density (ρ) of each pixel corresponding to bone was calculated from the CT images, using the standard hydroxyapatite calibration phantom to convert CT Hounsfield units to mineral bone density. The modulus of elasticity for trabecular bone was derived using the Rice *et al.*⁶ relationship:

$$E = 0.82\rho^2 + 0.07 \quad (1)$$

and the modulus for cortical bone was derived using the Snyder *et al.*⁷ relationship,

$$E = 21.91\rho - 23.5 \quad (2)$$

Where the transition from trabecular bone to cortical bone was assumed to occur at an apparent density of 1.1 g cm⁻³. EA, EI and GJ were calculated using the following formulae:

$$EA = \int E(\rho)da \quad (3)$$

$$EI = \int E(\rho)y^2da \quad (4)$$

$$GJ = \int G(\rho)(x^2 + y^2)da \quad (5)$$

where x and y are the distances to the neutral axis of the transaxial cross-section, and da is the pixel area.

The cross-section through the affected bone that had the lowest rigidity was considered the weakest link and was assumed to govern the failure behavior of the entire bone. However, this does not mean that CTRA can predict the exact failure load or pinpoint the exact location of an impending fracture. On the contrary, CTRA seeks to determine a fracture risk threshold whole bone using simple and reproducible measures.

Quantitative computed tomography (QCT) can only estimate the mineral material properties that can be resolved at the apparent density level and cannot identify changes in the extracellular matrix that are not related to mineralization. However, it has been previously established that bone tissue mineral density alone is not a strong indicator of the macroscopic mechanical behavior of bone.⁸ Furthermore, it is the minimum bone volume fraction (a measure of structural organization) that governs the mechanical behavior of normal and osteoporotic bone and even of metastatic cancer to bone.

Prediction of Fracture Risk Using Composite Beam Theory in Preclinical Studies

Several studies sought to determine the efficacy and performance of *ex vivo* fracture risk prediction using composite beam theory. The research strategy for all of them is essentially the same: the material and geometric properties of a bone specimen were determined using one of several imaging modalities and the structural rigidities of the sample for different loading modes were calculated using composite beam theory. The axial, bending and torsional rigidities then served as the predicted rigidity values and were correlated to the actual failure load as determined by mechanical testing under uniaxial tension, four-point bending and torsional loading. CTRA is the name given to such an approach when the noninvasive measurement of the specimen's material and geometric properties are acquired with QCT or micro-computed tomography (μ CT).

Whealan *et al.*,⁵ expanding on the work of Windhagen *et al.*,⁹ used the composite beam theory approach to predict the failure loads of human vertebrae with simulated lytic defects using QCT and dual-energy X-ray absorptiometry (DXA). Axial and bending rigidities were calculated from the image data, and a concordance correlation was performed to determine the association between the predicted failure load and the actual

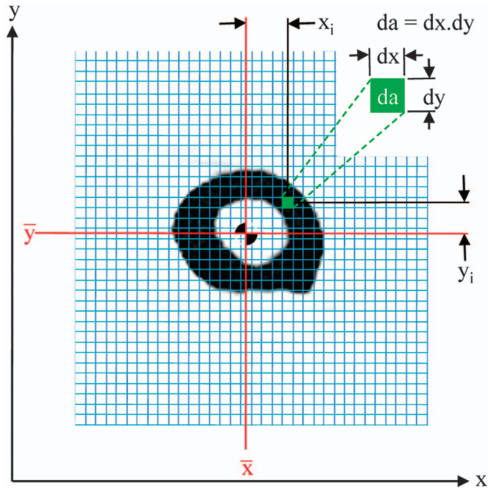


Figure 1 Axial (EA), bending (EI) and torsional (GJ) rigidity were calculated, with the use of the indicated algorithms, from transaxial computed tomography images of the affected and contralateral, unaffected bone. The ratio of the rigidity of the affected bone normalized by that of the contralateral limb at a homologous cross-section was calculated. The bone was predicted to be at risk of fracture if EA, EI or GJ was $\leq 65\%$ of that on the contralateral side ($da = \text{pixel size}$).¹⁷

Table 1 Dependence of linear regression on shape of defect for each imaging mode (QCT, DXA and MRI) by Hong *et al.*¹⁰

Imaging Mode	Mechanical testing mode	Aspect ratio (L/d)	Slope	R ²	Student's t-test on slope
QCT	Tension	1	3790	0.983	$P < 0.05$
		2	3200	0.938	
	Bending	1	1.32	0.949	$P < 0.05$
DXA	Tension	1	3280	0.953	$P < 0.05$
		2	2690	0.934	
	Bending	1	104	0.925	$P > 0.20$
MRI	Tension	1	6150	0.951	$P < 0.05$
		2	4670	0.89	
	Bending	1	2.0	0.918	$P > 0.20$
Torsion	1	1.72	0.538	$P < 0.05$	
	2	2.5	0.717		
Torsion	1	2.5	0.717	$P < 0.05$	
	2	3.5	0.913		

Abbreviations: DXA, dual-energy X-ray absorptiometry; MRI, magnetic resonance imaging; QCT, quantitative computed tomography.

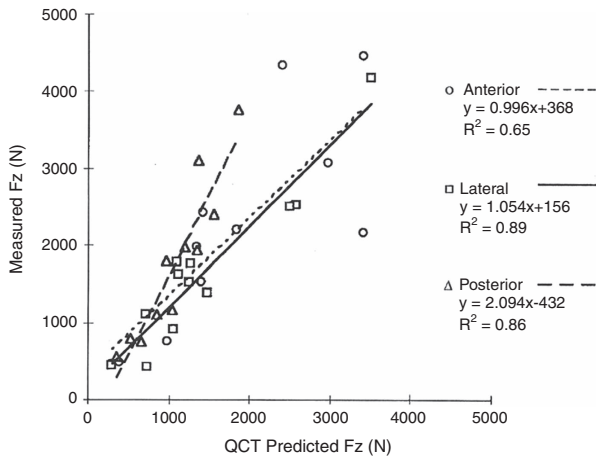


Figure 2 The slope of the regression line for the correlation between the quantitative computed tomography (QCT)-predicted and the measured failure loads (F_z) was dependent on defect location ($P = 0.023$). Although the overall regression was good ($R^2 = 0.69$), the correlative fit can be improved if confounding variables are considered.⁵

failure load as determined by mechanical testing. The authors demonstrated that defect geometry alone was a poor predictor of failure as the measured failure loads for the specimens had a large dispersion (coefficient of variation = 63%) in spite of a constant defect area. CTRA-derived measures of rigidity explained between 65 and 89% (overall $R^2 = 0.69$) of load failure variation, depending on the relative position of the defect (**Figure 2**). Furthermore, the failure loads calculated with the use of CTRA predicted the measured failure load on a one-to-one basis with a good correlation with the line $y = x$ ($r_c = 0.74$) (**Figure 2**). BMD and DXA-derived axial rigidity analogs also correlated well with the measured failure load ($R^2 = 0.72$ and 0.71, respectively). However, proper structural rigidities could not be calculated using DXA, as this technique is unable to evaluate the cross-sectional geometry of bone.

Hong *et al.*¹⁰ reported the first study of yield load prediction using composite beam theory on trabecular bone. Cylindrical cores of trabecular bone were harvested from the vertebral bodies of whale spines, and defects were simulated with through-holes of varying sizes and shapes. Structural rigidities were calculated using the material and geometric properties provided by QCT, DXA and magnetic resonance imaging (MRI). This study found that the axial, bending and torsional rigidities of homogeneous cores of trabecular bone with simulated defects—measured non-invasively by QCT, DXA or MRI in conjunction with composite beam theory—correlated highly with the corresponding yield loads in uniaxial tension, four-point bending and torsion (**Table 1**). LBC of the entire core was directly proportional to the measured bone rigidities at the weakest cross-section through the core containing the defect. The differences in the slopes of the linear regressions between yield load and minimum cross-sectional rigidity calculated using QCT or MRI data reflected the inherent differences between the direct and indirect measurements of bone density using QCT and MRI, respectively. A third study was performed to determine the predictive performance of CTRA in an animal model of long-bone osseous defects.¹¹ Simulated lytic lesions of varying sizes and locations were created on the femora of Sprague–Dawley rats, and torsional failure loads were predicted with the use of μ CT and DXA. In this study, CTRA described 85% of the variation in failure loads (**Figure 3a**), whereas DXA could only account for 32% of failure variation (**Figure 3b**). In accordance to the results of Whealan *et al.*,⁵ the slope and y-intercept of the failure load regression line were not different from those of the line $y = x$ ($P = 0.46$), suggesting that the correlation between the CTRA-based failure load and actual failure load, as assessed by mechanical testing, occurred on a one-to-one basis.

Given the ability of CTRA to detect structural and material changes within trabecular and cortical bone, Smith *et al.*¹² hypothesized that CTRA could accurately predict the failure loads of rat femora affected by metabolic diseases—namely, post-menopausal bone loss and renal osteodystrophy with

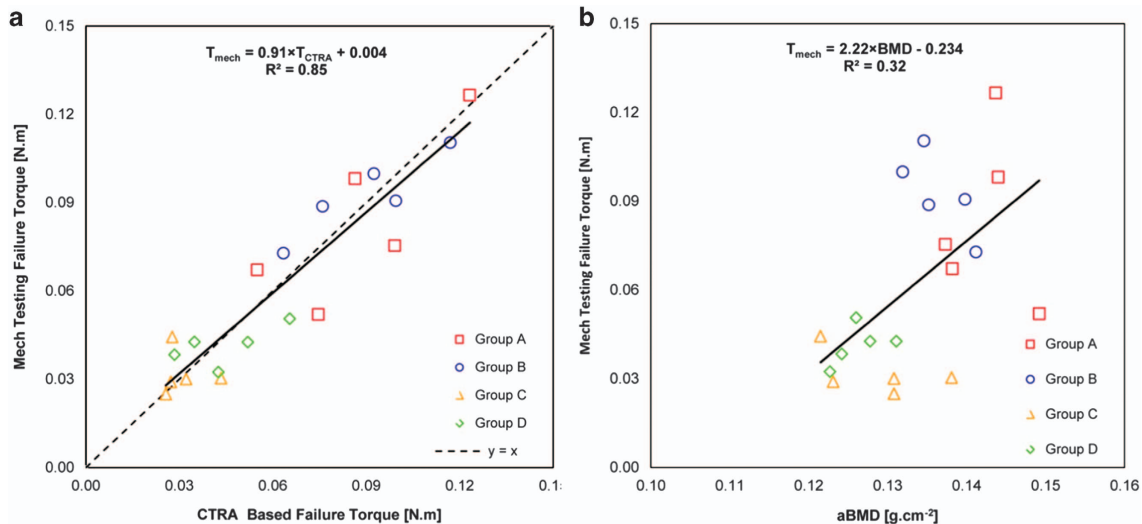


Figure 3 (a) Linear regression of failure torque as assessed by CTRA versus mechanical testing and (b) linear regression of failure torque as assessed by mechanical testing versus DXA-based aBMD.¹¹

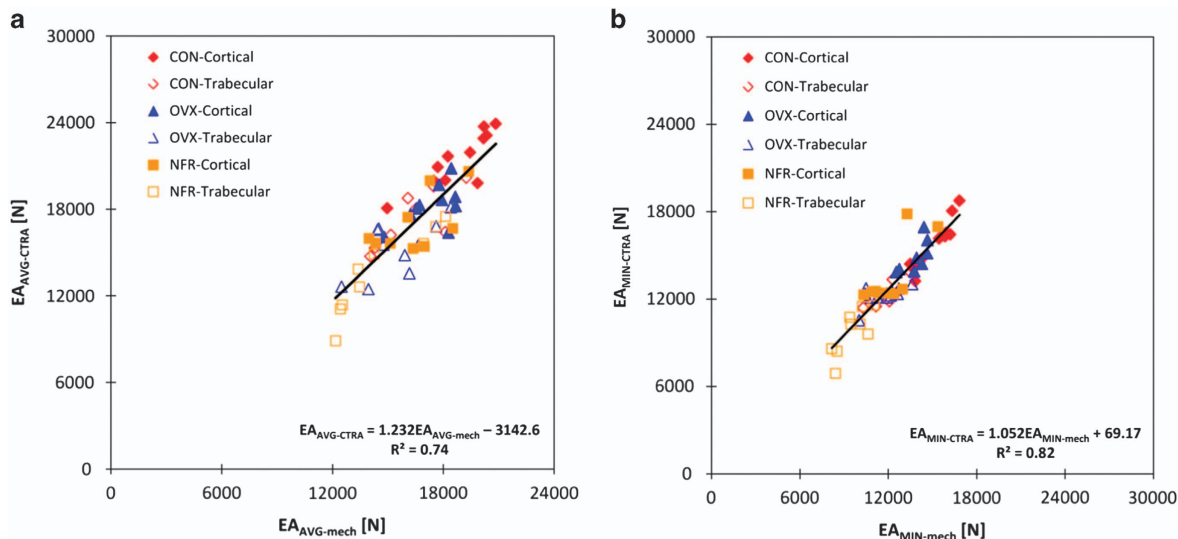


Figure 4 (a) Linear regression of the average axial rigidity (EA) as assessed by CT structural rigidity analysis ($EA_{AVG-CTRA}$) and mechanical testing ($EA_{AVG-mech}$). CON, control; OVX, ovariectomized; NFR, partially nephrectomized. (b) Linear regression of the minimum axial rigidity (EA) as assessed by CT structural rigidity analysis ($EA_{MIN-CTRA}$) and mechanical testing ($EA_{MIN-mech}$).¹²

secondary hyperparathyroidism. Again, axial rigidity measured noninvasively by CTRA was well correlated with the results from mechanical testing. Average and minimum axial rigidities showed a strong correlation with mechanical testing results ($R^2 = 0.74$ and 0.82 , respectively; **Figure 4**). When average axial rigidity for the specimens was used to predict failure loads, the slope of the linear regression was 1.23 and the y-intercept offset was 3142; average axial rigidity consistently overestimated bone rigidity. On the other hand, when minimum axial rigidity was used, the slope of the linear regression was 1.05 and the y-intercept offset was 69, indicating that CTRA was correlated without skewness with mechanical testing results over the full range of the values tested. There were no significant difference between axial rigidity as determined by CTRA and mechanical testing ($P > 0.13$).

Structural rigidity analysis has also been used to evaluate the progression of the fracture healing process by quantifying the

mechanical properties of fracture calluses.¹³ Rats with femoral critical defects received human BMP-2 complimentary DNA in an adeno-viral vector at various time points to accelerate fracture healing. The femora were harvested 56 days after the injury and were subjected to μ CT imaging. CTRA-based average torsional rigidity was moderately correlated with torsional rigidity assessed from mechanical testing results ($R^2 = 0.63$; **Figure 5a**). This correlation improved significantly when the CTRA-based minimum torsional rigidity was correlated to the mechanical testing-based results ($R^2 = 0.81$; **Figure 5b**). No significant differences were observed between the CTRA-based minimum torsional rigidity and those obtained from mechanical testing based on paired *t*-test analysis ($P = 0.43$). On the basis of mechanical testing results, femora with defects undergoing BMP-2 treatment regained 5–166% of their torsional strength when compared with their respective contralateral specimens. The CTRA-based

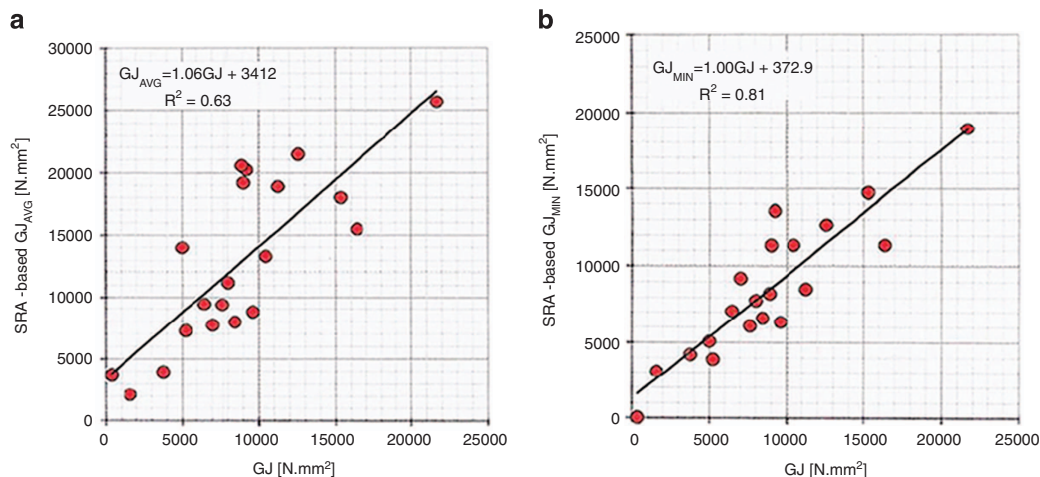


Figure 5 (a) Average mechanical testing-based versus CT-based GJ correlation and (b) Minimum mechanical testing-based versus CT-based GJ correlations.¹³

minimum torsional rigidity placed this ratio at 2–163%, whereas the CT-based average torsional rigidity resulted in a range of 15–218%.

The data from Smith *et al.*¹² and Nazarian *et al.*¹³ suggest that minimum rigidity is more accurate compared with average rigidity in predicting the failure loads of the specimens as determined by mechanical testing. This corresponds to expected behavior, where the weakest point, and not the average strength, determines the failure of a beam under angular displacement.

Direct Comparisons of CT-based and Finite Element Analysis

Rennick *et al.*¹⁴ used a rat model of simulated tibial osteolytic defects in order to compare the CT-based and finite element analysis (FEA) fracture risk methodologies. The tibiae were randomly assigned to four equal groups; three of the groups included a simulated defect at various locations and the fourth group served as an intact control. μ CT was used to assess bone structural rigidity properties and to provide three dimensional (3D)-model data for generation of the FEA models for each specimen. Compressive failure loads calculated using CT-based were well correlated to failure loads recorded in mechanical testing, and this model accounted for 96% of the variation in failure load ($R^2 = 0.96$, $P < 0.01$). On the other hand, failure loads calculated with FEA were less accurate for this model accounting for 75–90% of the variation in failure loads (elastic isotropic model: $R^2 = 0.75$, $P < 0.01$ /elastic transversely isotropic model: $R^2 = 0.90$, $P < 0.01$). The results of this study indicated that CT-based analysis of bone strength correlates well with both FEA and compression testing.

Anez-Bustillos *et al.*¹⁵ directly compared the accuracy of CT-based and FEA to estimate failure loads in human cadaveric femora with simulated lytic defects. They conducted mechanical test to failure as a gold standard. Prior to testing, FEA models were generated and CT-based was performed to obtain axial and bending rigidity measurements. Overall, the axial and bending rigidities obtained through CT-based correlated well with the load capacity obtained from mechanical testing. The coefficients of determination for the femurs were 0.82 for EA and 0.86 for EI (< 0.001 for all cases). The simulated FEA models accurately predicted the failure load of the intact as well as the

metastatic femurs as measured in the experiments ($R^2 = 0.89$ and $P < 0.001$). Kendall rank correlation coefficients between the FEA rankings and the CT-based rankings showed moderate to good correlations. No significant differences in prediction accuracy were found between the two methods.

Unlike previously proposed radiographic guidelines, both methods are able to deliver objective predictions while considering important biomechanical aspects of the bone, being a 3D structure governed by its material and geometric properties; even if these are affected by the presence of a lytic lesion. Both techniques are based on QCT imaging, but the sophisticated and relatively complex finite element (FE) software required asks for a certain level of expertise as well as background in structural mechanics.¹⁶ In addition, computational times differ considerably between the two methods. Although generating and running the FE simulations in these studies took about 8 h per sample, CT-based took only ~ 30 min. The CT-based software is intentionally designed to be simple and readily useable on a regular computer. Furthermore, additional modeling knowledge is needed for generating the FE models. For those reasons, one would choose CT-based analysis. In contrast, FE simulations would be more suitable for the implementation of complex loading conditions.

Validation of the Technique in Clinical Studies

Current radiographic guidelines for predicting fracture risk in children with a benign skeletal lesion are neither sensitive nor specific.¹⁶ Snyder *et al.* retrospectively studied a cohort of 36 patients with a benign skeletal lesion to establish thresholds for CT-based-derived metrics to discriminate lesions at risk for fracture.¹⁶ CT-based was performed to calculate the axial, bending and torsional rigidities along the length of the bone containing the lesion and from homologous cross-sections through the contralateral, normal bone. At each cross-section, the ratio of the structural rigidity of the affected bone divided by that of the normal, contralateral bone was determined. A 35% reduction in structural rigidity discriminated fracture from non-fracture cases with 100% sensitivity and 94% specificity. The cutoff value was determined for a combination of EI and GJ and was derived on the basis of the multivariate model with the use of maximum likelihood estimation. In contrast, plain radiographic

Table 2 Sensitivity and specificity details for all fracture prediction models used in noninvasive prediction of fracture risk in patients with metastatic cancer to the spine by Snyder *et al.*²⁴

Model	Cuff value	Sensitivity (%)	Specificity (%)	AUC	CI of AUC (m ²)		P
					Lower bound	Upper bound	
RC	—	100	20	0.60	0.46	0.74	0.25
LBC (N)	1607.5	100	44	0.82	0.73	0.91	0.001
EI (N m ²)	154640	100	53	0.80	0.72	0.89	0.001
EA (N)	726	100	55	0.77	0.68	0.87	0.002
LBC/BMI (N kg m ⁻²)	46.5	100	70	0.84	0.78	0.93	<0.001

Abbreviations: AUC, area under the curve; BMI, body mass index; CI, confidence interval; EA, axial rigidities; EI, bending rigidities; LBC, load-bearing capacity; RC, radiographs criteria.

criteria demonstrated 28–83% sensitivity and 6–78% specificity.

In a follow-up study, Leong *et al.*¹⁷ conducted a prospective study of children with benign appendicular skeletal lesions. CTRA was performed to establish the rigidity of the affected bone in comparison with the contralateral, unaffected bone and interpreted using the threshold determined by Snyder *et al.*¹⁶ The specificity of two methods, CTRA and plain radiographic criteria¹⁸ (lesion length ≥ 3.3 cm, width ≥ 2.5 cm or cortical involvement $> 50\%$), for the prediction of pathologic fracture was determined in a cohort of 34 patients who did not receive surgical treatment during a 2-year follow-up period. Overall, the specificity of CTRA was 97% (95% confidence interval (CI) = 83–100%), with the method correctly predicting that a bone containing an osteolytic lesion would not fracture when the patient engaged in activities of daily living. In comparison, the criteria based on plain radiographs had a specificity of only 12% (95% CI) = 4–28%) for the prediction that a bone containing an osteolytic lesion would not fracture. The sensitivity of CTRA was not evaluated because of ethical concerns: most surgeons felt obligated to treat a bone lesion if CTRA predicted that the affected bone was at increased risk for fracture.

Lesion size has often been used as a predictor of vertebral fracture risk in patients with osteolytic metastases to the spine, but this parameter only accounts for 50% of the variation in vertebral body strength.^{19,20} Furthermore, 30–75% of the bone must be destroyed before an osteolytic lesion is detectable on a plain radiograph, and the strength of the affected bone is already reduced 50–90% by the time metastasis is evident radiographically.^{16,21,22} In order to accurately diagnose impending vertebral collapse, Taneichi *et al.*²³ developed a fracture prediction method empirically based on a retrospective review of patients with spinal metastases that fractured: using multivariate logistic regression analysis they estimated the risk of a vertebral fracture as a function of the size and the location of the lesion within the vertebra. Briefly, transaxial CT images were acquired through the affected vertebrae to establish the probability that a vertebra containing an osteolytic metastasis involving at least 25–45% of its cross-section would fracture, depending on the type of vertebra (thoracic versus lumbar), percentage of tumor occupancy and the location of the osteolytic lesion within the vertebra.

To validate the use of CTRA for the prediction of vertebral fractures Snyder *et al.*²⁴ conducted a prospective study of 94 women with vertebral metastatic breast cancer comparing the performance of CTRA to Taneichi *et al.*²³ empirically derived fracture risk prediction model. Both methods proved to be

100% sensitive in predicting the 11 fractures that occurred in the 4-month follow-up period. However, CTRA provided better specificity results, ranging from 44 to 70% (Table 2). LBC normalized by body mass index provided the best specificity among the predicting variables.

Impact on Clinical Decision Making

A survey study of physicians from the specialties of orthopedic oncology, radiation oncology and musculoskeletal radiology was conducted to establish the impact of CTRA on clinicians' fracture risk assessment and treatment recommendations for simulated clinical scenarios of metastatic bone disease.²⁵ Eighteen clinical vignettes were presented to the participants under three separate scenarios in a random order: (i) no CTRA input (baseline scenario); (ii) CTRA input suggesting increased risk of fracture; and (iii) CTRA input suggesting decreased risk fracture. CTRA had a significant, albeit small, impact on fracture risk assessment and on treatment planning when compared with the baseline scenario. Nevertheless, CTRA did not increase inter-observer agreement regarding treatment recommendations when compared with the baseline scenario (multi-rater kappa = 0.41 and 0.43, respectively). The largest effect of CTRA on fracture risk assessments and treatment recommendations was observed during subgroup analyses in orthopedic oncologists. This led the authors to conclude that CTRA may hold more credibility among physicians with knowledge in the field of skeletal biomechanics. This study provided an initial measure of the impact of CTRA on clinical decision making. The role of additional education and training regarding CTRA among this group of physicians is yet to be determined.

Between 2009 and 2012, a multicenter, prospective study was conducted to identify factors that determine the treatment recommended by orthopedic oncologists for patients with appendicular skeletal metastasis. The purpose of this work was to evaluate prospectively whether CTRA was more accurate at predicting pathologic fractures than clinical and radiographic fracture risk assessments.²⁶ In addition, it aimed to evaluate whether inclusion of CTRA results could alter the treatment plan outlined by physicians. Orthopedic oncologists were asked to select a treatment plan for 124 patients based on their initial risk assessment using Mirels method.²⁷ Then, CTRA was performed on CT scans of the involved bones, and the results were provided to the enrolling physicians, who were asked to reassess their treatment plan. The pre- and post-CTRA treatment plans were compared with identify cases, where treatment plan could be changed as a result of the CTRA results.

The patients who did not undergo prophylactic stabilization by the treating physician were followed up over a 4-month period, and pathologic fractures at the lesions sites were recorded at incidence or at subsequent visits.

Modeling the physician's post-CTRA plan revealed that CTRA, pain level and primary source of metastasis were significant predictors of the post-CTRA plan (Table 3). On the basis of this model, CTRA was the most significant predictor of the physicians' plan (odds ratio = 118.1; 95% CI: 25.0–557.2), meaning that after controlling for the rest of the predictors, a positive CTRA report increased the probability of assigning a patient to surgery, and, on the basis of the lower limit of the

confidence interval, physicians were at least 25 times more likely to recommend surgery than no surgery after receiving a positive CTRA report.

Seven new fractures, all at the lesion sites, were reported in the follow-up period in seven different patients. All new fractures were correctly predicted to fracture (100% sensitive) using the CTRA method. Of the 58 lesions that did not fracture, CTRA predicted six of them to fracture (90% specific). Only five of the seven new fractures were correctly predicted to fracture (71% sensitive) using the Mirels method. Of the 58 lesions that did not fracture, Mirels method predicted 29 of them to fracture (50% specific). The sensitivity and specificity of the CTRA method were significantly better than those of the Mirels method ($P = 0.002$).

Table 3 Pre- and Post-CTRA modeling results for the multicenter study on patients with appendicular skeletal lesions²⁶

Covariate	Pre-CTRA		Post-CTRA	
	Wald χ^2 -value	P	Wald χ^2 -value	P
Age	0.9	0.35	0.1	0.82
Source of mets ^a	0.89	0.12	11.4	0.04 ^b
Lesion size	4.3	0.04 ^b	0.1	0.77
Lesion location	2.9	0.09	1.5	0.23
Lesion type	13.3	<0.001	3.1	0.08
Pain level	24.1	<0.001	14.5	<0.001
SF-36 PCS	1.3	0.26	2.4	0.13
CTRA	—	—	36.4	<0.001

Abbreviations: CTRA, CT- based rigidity analysis; PCS, physical component summary.

^aSource of mets refers to the primary cancer type in the patient. The Wald χ^2 values allow for a relative comparison of the predictors in terms of their importance, as used to test the true value of a given parameter based on the sample estimate. For the pre-CTRA case, pain is the most significant contributor followed by lesion type and size. For the post-CTRA case, CTRA result is the most significant contributor followed by pain and source of mets. ^bStatistically significant.

Determination of Bone Structural Properties with CTRA in Hutchinson–Gilford Progeria

CTRA was essential in determining Hutchinson–Gilford Progeria (HGPS) as a skeletal dysplasia, affecting the structural geometry of the appendicular skeleton rather than a premature loss of bone mass.^{28,29} A cohort of 26 children with HGPS was enrolled and areal bone mineral densities (aBMDs) of the total body and lumbar spine were measured at one time point by DXA. Measurements were compared with age- and gender-matched controls. In addition, CTRA was performed using transaxial pQCT images acquired at four sites along the radius, and the resulting structural rigidities and volumetric BMD (vBMD) were compared with 57 age- and gender-matched controls.

Unadjusted, DXA-derived Z-scores of aBMD were low (< -2 s.d.) in all children with HGPS; yet, fracture rates were low in the face of normal daily physical activity. Adjustments for

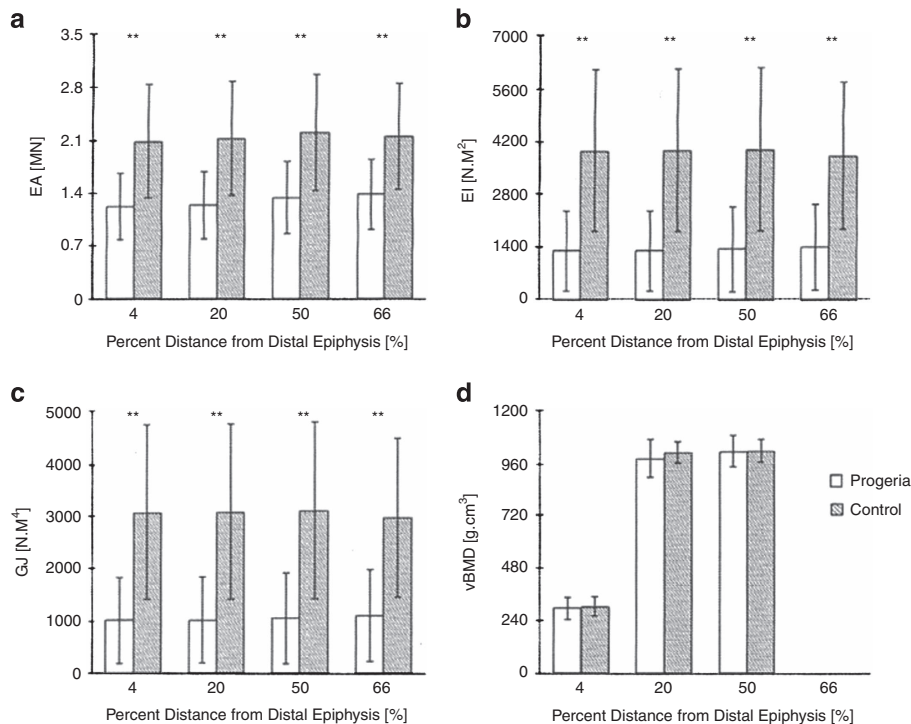


Figure 6 Differences in skeletal rigidity ((a) Axial (EA), (b) bending (EI), (c) torsional (GJ) and (d) volumetric bone mineral density (vBMD)) in patients with HGPS versus healthy controls.²⁸ $**P < 0.0001$.

bone age did not significantly influence aBMD Z-scores, because bone age was variable and overall was not significantly different from chronologic age. However, DXA provides only a 2D measurement of apparent bone density; it can be confounded in the context of a disease where extremely small size and/or altered bone age may influence the analysis. Comparing DXA measures of aBMD of patients with HGPS with reference data matched for chronologic age resulted in overestimation of deficits in skeletal mineral mass.

Structural rigidity variables were markedly abnormal at all sites compared with the age- and gender-matched normal control group (**Figures 6a–c**). Axial rigidity of the radii of the HGPS patients was on average 40% lower than those of control subjects ($P < 0.0001$ at all four radial sites). Bending and torsional rigidities of the radii of the HGPS patients were on average 66% lower compared with controls ($P < 0.0001$) at all four radial sites. However, total vBMD measured by QCT was comparable with that of the normal controls throughout the radius (**Figure 6d**). Therefore, HGPS appears to affect primarily the structural geometry, suggestive of a skeletal dysplasia.

Conclusion

There is an unmet clinical need to better identify which patients are at substantial fracture risk, so that appropriate intervention can be initiated before catastrophic failure occurs. Currently, there is no proven sensitive or specific method for predicting pathologic fractures of bones with osseous neoplasms. Decisions regarding the management of bone lesions are currently based on geometric measurements of the bone, the defect or both. The results of several studies suggest that better treatment plans can be made by predicting failure (and, by extension, by predicting fracture) with the use of QCT-derived structural properties coupled with composite beam theory CTRA.

The body of work presented in this review shows that CTRA-derived indices are strongly correlated with the measured mechanical failure loads in *ex vivo* models of metastatic bone disease. Similarly, CTRA assessments of bone strength correlate with advanced modeling techniques such as FEA. Finally, by assessing fracture prediction through benign skeletal lesions and malignant neoplasms, CTRA has demonstrated to be a significant predictor of fracture occurrence and has demonstrated improved diagnostic performance over standard methods of fracture risk assessment (plane radiographic criteria and empirically derived multivariate logistic regression models).

The load-carrying capacity of bone depends on many factors that are not represented by radiographic criteria based on lesion size alone. The critical parameters that determine the LBC of a bone containing a lytic lesion include the amount of bone loss, the cross-sectional structural geometry of the bone, the material properties of the remaining bone tissue, the location of the lesion with respect to the applied loads and the loading mode.^{4,5,10} The advantage of our analysis of structural rigidity with QCT is that it reflects changes in both the material properties of the bone tissue and the bone cross-sectional geometry for any bone or lesion. BMD alone, which is often used to predict the risk of an osteoporotic fracture in the elderly, does not reflect how the bone mineral is distributed in space, which determines the load-carrying capacity of the bone.

One limitation of CTRA performed in the clinical setting is that it requires a normal contralateral bone for comparison: because

of the diverse range of patients' activities, the actual loads applied to the bones are unknown. Therefore, the current approach involves comparing the structural properties of the affected bone with those of the contralateral, normal bone at homologous cross-sections to calculate the reduction in the load-carrying capacity of the affected bone. Although individual differences of up to 13% can be observed, these differences are smaller compared with the 33% reduction in bending rigidity that has been established as the threshold for fracture occurrence. If the other limb is also pathologically involved, as seen with polyostotic fibrous dysplasia, osteogenesis imperfecta, metabolic bone disease and metastatic cancer, one cannot assume that the contralateral limb provides an appropriate internal control. In that case, the fracture risk must be calculated by comparing the estimated load applied to the bone for a specific activity to the calculated failure load of the bone. Another limitation of CTRA is that it exposes the patient to relatively large doses of radiation, so that repeated measurements are less desirable in children.

CTRA is a powerful, robust and noninvasive tool, based on fundamental principles of engineering mechanics, and can be used to reliably identify patients at risk of sustaining a pathologic fracture. However, and because of the novelty of the technique, there are no clinical guidelines or criteria to determine which patients should undergo CTRA. Therefore, at the moment, this decision should be guided by clinical judgment in a context where the benefits of prophylactic fixation outweigh the risks of such an invasive procedure. Increased awareness of clinicians to CTRA, including its underlying methodology to study bone structural characteristics, may establish this methodology as a uniform guideline across specialties to assess fracture risk and to plan treatment for patients afflicted with osseous lesions.

Conflict of Interest

The authors declare no conflict of interest.

Acknowledgements

We acknowledge the Musculoskeletal Tumor Society (BDS), Orthopaedic Research and Education Foundation (AN), Boston Children's Hospital Orthopaedic Surgery Foundation (BDS) and the National Institutes of Health (R01 CA40211) (BDS), T32 COMET Program (AR055885; AN), LRP (L30 AR056606; AN) and (R01 AR056212) for providing financial support towards this project. They would also like to acknowledge all co-authors who have contributed significantly to the compendium of work presented here and all patients who have participated in our studies.

References

1. Riggs B, Melton 3rd LJ. The worldwide problem of osteoporosis: insights afforded by epidemiology. *Bone* 1995;17(5 Suppl):505S–511SS.
2. Cummings SR. Epidemiology of osteoporotic fractures. In: Genant HK (ed) *Osteoporosis Update 1987*. Radiology Research and Education Foundation: San Francisco, 1987, pp 7–12.
3. Melton 3rd LJ. Excess mortality following vertebral fracture. *J Am Geriatr Soc* 2000;48:338–339.
4. Hipp JA, Springfield DS, Hayes WC. Predicting pathologic fracture risk in the management of metastatic bone defects. *Clin Orthop Relat Res* 1995;312:120–135.
5. Whealan KM, Kwak SD, Tedrow JR, Inoue K, Snyder BD. Noninvasive imaging predicts failure load of the spine with simulated osteolytic defects. *J Bone Joint Surg Am* 2000;82:1240–1251.

6. Rice JC, Cowin SC, Bowman JA. On the dependence of the elasticity and strength of cancellous bone on apparent density. *J Biomech* 1988;**21**:155–168.
7. Snyder S, Schneider E. Estimation of mechanical properties of cortical bone by computed tomography. *J Orthop Res* 1991;**9**:422–431.
8. Nazarian A, von Stechow D, Zurakowski D, Muller R, Snyder BD. Bone volume fraction explains the variation in strength and stiffness of cancellous bone affected by metastatic cancer and osteoporosis. *Calcif Tissue Int* 2008;**83**:368–379.
9. Windhagen HJ, Hipp JA, Silva MJ, Lipson SJ, Hayes WC. Predicting failure of thoracic vertebrae with simulated and actual metastatic defects. *Clin Orthop Relat Res* 1997;**344**:313–319.
10. Hong J, Cabe GD, Tedrow JR, Hipp JA, Snyder BD. Failure of trabecular bone with simulated lytic defects can be predicted non-invasively by structural analysis. *J Orthop Res* 2004;**22**:479–486.
11. Entezari V, Basto PA, Vartanians V, Zurakowski D, Snyder BD, Nazarian A. Non-invasive assessment of failure torque in rat bones with simulated lytic lesions using computed tomography based structural rigidity analysis. *J Biomech* 2011;**44**:552–556.
12. Smith MD, Baldassarri S, Anez-Bustillos L, Tseng A, Entezari V, Zurakowski D *et al*. Assessment of axial bone rigidity in rats with metabolic diseases using CT-based structural rigidity analysis. *Bone Joint Res* 2012;**1**:13–19.
13. Nazarian A, Pezzella L, Tseng A, Baldassarri S, Zurakowski D, Evans CH *et al*. Application of structural rigidity analysis to assess fidelity of healed fractures in rat femurs with critical defects. *Calcif Tissue Int* 2010;**86**:397–403.
14. Rennick JA, Nazarian A, Entezari V, Kimbaris J, Tseng A, Masoudi A *et al*. Finite element analysis and computed tomography based structural rigidity analysis of rat tibia with simulated lytic defects. *J Biomech* 2013;**46**:2701–2709.
15. Anez-Bustillos L, Derikx LC, Verdonshot N, Calderon N, Zurakowski D, Snyder BD *et al*. Finite element analysis and CT-based structural rigidity analysis to assess failure load in bones with simulated lytic defects. *Bone* 2014;**58**:160–167.
16. Snyder BD, Hauser-Kara DA, Hipp JA, Zurakowski D, Hecht AC, Gebhardt MC. Predicting fracture through benign skeletal lesions with quantitative computed tomography. *J Bone Joint Surg Am* 2006;**88**:55–70.
17. Leong NL, Anderson ME, Gebhardt MC, Snyder BD. Computed tomography-based structural analysis for predicting fracture risk in children with benign skeletal neoplasms: comparison of specificity with that of plain radiographs. *J Bone Joint Surg Am* 2010;**92**:1827–1833.
18. Arata MA, Peterson HA, Dahlin DC. Pathological fractures through non-ossifying fibromas. Review of the Mayo Clinic experience. *J Bone Joint Surg Am* 1981;**63**:980–988.
19. McGowan DP, Hipp JA, Takeuchi T, White 3rd AA, Hayes WC. Strength reductions from trabecular destruction within thoracic vertebrae. *J Spinal Disord* 1993;**6**:130–136.
20. Silva MJ, Hipp JA, McGowan DP, Takeuchi T, Hayes WC. Strength reductions of thoracic vertebrae in the presence of transcortical osseous defects: effects of defect location, pedicle disruption, and defect size. *Eur Spine J* 1993;**2**:118–125.
21. Edelstyn GA, Gillespie PJ, Grebbell FS. The radiological demonstration of osseous metastases. Experimental observations. *Clin Radiol* 1967;**18**:158–162.
22. Tubiana-Hulin M. Incidence, prevalence and distribution of bone metastases. *Bone* 1991;**12**(Suppl 1):S9–S10.
23. Taneichi H, Kaneda K, Takeda N, Abumi K, Satoh S. Risk factors and probability of vertebral body collapse in metastases of the thoracic and lumbar spine. *Spine* 1997;**22**:239–245.
24. Snyder BD, Cordio MA, Nazarian A, Kwak SD, Chang DJ, Entezari V *et al*. Noninvasive prediction of fracture risk in patients with metastatic cancer to the spine. *Clin Cancer Res* 2009;**15**:7676–7683.
25. Nazarian A, Entezari V, Villa-Camacho JC, Zurakowski D, Katz JN, Hochman M *et al*. Fracture Prediction and Treatment Planning in Patients with Skeletal Metastasis: A Survey Study to Evaluate The Impact of CT-based Rigidity Analysis on Decision Making 2014.
26. Nazarian A, Entezari V, Zurakowski D, Calderon N, Hipp JA, Villa-Camacho JC *et al*. Improvements in Treatment Planning and Fracture Prediction in Patients with Skeletal Metastasis with CT-based Rigidity Analysis 2014. Available at: <http://www.wccm-eccm-ecfd2014.org/admin/files/fileabstract/A4219.pdf>.
27. Mirels H. Metastatic disease in long bones. A proposed scoring system for diagnosing impending pathologic fractures. *Clin Orthop Relat Res* 1989;**249**:256–264.
28. Gordon CM, Gordon LB, Snyder BD, Nazarian A, Quinn N, Huh S *et al*. Hutchinson-Gilford progeria is a skeletal dysplasia. *J Bone Miner Res* 2011;**26**:1670–1679.
29. Gordon LB, Kleinman ME, Miller DT, Neuberger DS, Giobbie-Hurder A, Gerhard-Herman M *et al*. Clinical trial of a farnesyltransferase inhibitor in children with Hutchinson-Gilford progeria syndrome. *Proc Natl Acad Sci USA* 2012;**109**:16666–16671.